chemistry

MDPI

Article

Synthesis of Glycoluril Dimers with the Ability to Form Polymeric Self-Associates in Water

Jan Sokolov [1,2] and Vladimír Šindelář [1,2,*]

[1] Department of Chemistry, Faculty of Science, Masaryk University, Kamenice 5, 62500 Brno, Czech Republic; sokolov@mail.muni.cz
[2] RECETOX, Faculty of Science, Masaryk University, Kamenice 5, 62500 Brno, Czech Republic
* Correspondence: sindelar@chemi.muni.cz

Abstract: Supramolecular self-assembly in water resulting in polymeric structures is emerging because of its potential in the preparation of adaptive materials with applications in biology and medicine. Here, we report the first example of host molecules based on glycoluril dimers, which self-associate into linear oligomers in water. The degree of polymerization for the resulting supramolecular aggregates was calculated using the isodesmic model and the Carothers equation. The model compound was prepared to enable a deeper understanding of the forces responsible for the self-association of the glycoluril dimer-based monomers in water.

Keywords: glycolurils; self-assembly; supramolecular polymers; binding in water

check for updates

Citation: Sokolov, J.; Šindelář, V. Synthesis of Glycoluril Dimers with the Ability to Form Polymeric Self-Associates in Water. *Chemistry* **2022**, *4*, 753–764. https://doi.org/10.3390/chemistry4030053

Academic Editor: Craig Rice

Received: 7 July 2022
Accepted: 25 July 2022
Published: 26 July 2022

Publisher's Note: MDPI stays neutral with regard to jurisdictional claims in published maps and institutional affiliations.

1. Introduction

Self-assembly is a spontaneous and reversible phenomenon that utilizes the ability of molecules to noncovalently interact with each other to produce supramolecular aggregates [1]. The assembly of viral capsids or DNA demonstrates the importance of this process in natural systems. On the other hand, supramolecular chemists use the self-assembly process to produce molecular cages or capsules as it allows one to reach such complex systems in relatively fewer steps than conventional synthesis [2]. In aqueous media, a typical example of self-assembly is the aggregation of amphiphilic compounds driven by hydrophobic forces. This includes common head/tail amphiphiles, which assemble into micelles or bilayers, as well as compounds with complementary hydrophobic areas, which assemble into discrete complexes [3].

Glycoluril is a versatile building block widely used in supramolecular chemistry for the construction of host molecules, including cucurbit[*n*]urils [4] and bambus[*n*]urils [5]. Many glycoluril-containing host molecules with the ability to self-assemble in organic non-polar solvents have been described [6,7]. However, the self-assembly of glycoluril-based molecules in competitive media such as water is reported to a much lesser extent. In this sense, acyclic containers composed of one to five glycoluril moieties connected by two rows of methylene bridges showed some promising results [8–12]. These containers are typically terminated with aromatic sidewalls, and their solubility in water is achieved by installing solubilizing substituents containing, for example, carboxyl or sulfonic groups [9,10,13]. In addition to their ability to act as supramolecular hosts for various guest molecules [14–18], glycoluril-based acyclic containers are known to self-associate into dimeric aggregates in water [19,20]. This process competes with guest encapsulation; therefore, it is undesirable for applications where strong host–guest binding is required, such as the use of acyclic oligomers to improve the solubility of hydrophobic drugs or to deactivate neuromuscular blocking agents and illicit recreational drugs [21,22]. For such purposes, dimerization was suppressed by placing charged (water solubilizing) groups on the aromatic sidewalls, causing the repulsion of these molecules. The aggregation of glycoluril-based acyclic containers in water resulting in large self-assembled structures has been reported sporadically [23,24].

Nolte et al. reported several examples of glycoluril-based clips, that self-assembled into nano-objects of different shapes as a result of a particularly hydrophobic effect. However, glycoluril derivatives with the ability to act as monomers for the formation of water-soluble supramolecular oligomers and polymers have not been described. In this work, we designed and synthesized compound **4** (Scheme 1) consisting of two connected glycoluril-based containers with the ability to self-associate in water. The formation of supramolecular oligomers induced by the self-association of **4** was investigated.

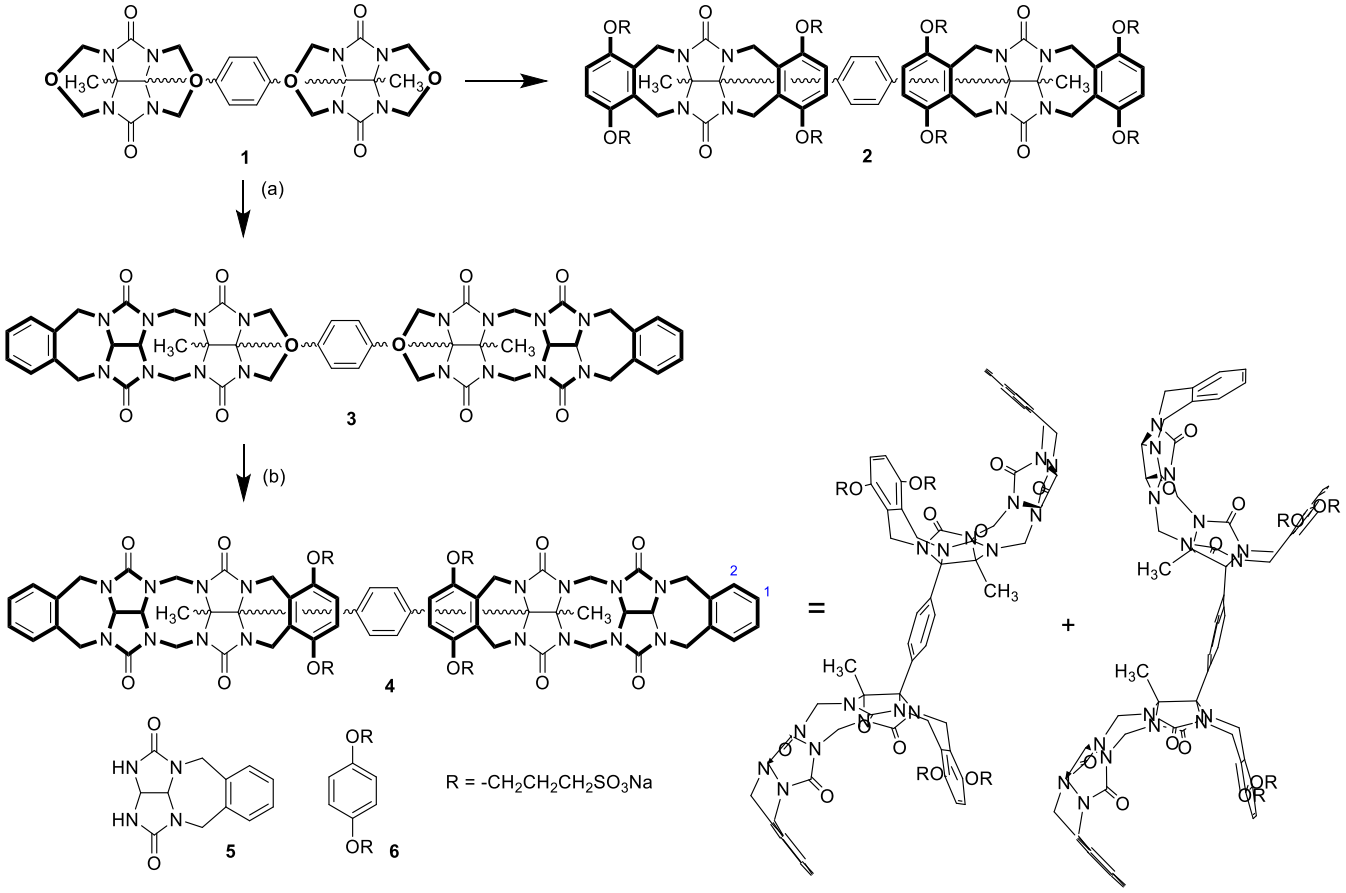

Scheme 1. Synthesis of previously reported clips **2** and a novel glycoluril derivative **4** with two binding sites. Both possible conformers of **4** are shown. For capped stick representations of conformers of **4** see Figure S20. Reaction conditions: (**a**) **5**, $MeSO_3H$, 60 °C, 4 h, 72%; (**b**) **6**, TFA/Ac_2O, 95 °C, 3 h, 45%.

2. Results and Discussion

The design of compound **4** was inspired by our previous work [25], in which we prepared host molecule **2** featuring two coupled glycoluril-based clips (Scheme 1). The ability of **2** to bind two cationic guests simultaneously in water was reported. However, host **2** had four sulfonate units on each of two connected clips, which prevented the self-association of its molecules. We envisioned, that substitution of the clips in **2** for glycoluril dimer motives in structure **4** might increase the self-association ability required for the formation of a supramolecular polymer. Glycoluril dimer motive was selected in favor of higher glycoluril oligomers as methylene-bridged glycoluril dimers terminated with aromatic side walls showed a higher tendency to self-associate [19,20,26] than monomeric clips [15,27,28], while the self-association of trimers or tetramers was only scarcely reported [10]. We suggested that each of the two glycoluril dimers of **4** should be terminated by xylylene units, but only one of these xylylenes should be further modified by sulfopropyl substituents. Sulfonate groups were necessary to solubilize **4** in water. On the other hand, the lack of solubilizing substituents on second xylylene units promises a higher tendency toward self-association. Indeed, molecular modeling showed that two molecules of **4** could undergo self-association

(Figure 1). As one molecule of clip **4** possesses two sites capable to self-associate, clip **4** is a promising building block for supramolecular polymers in aqueous solution.

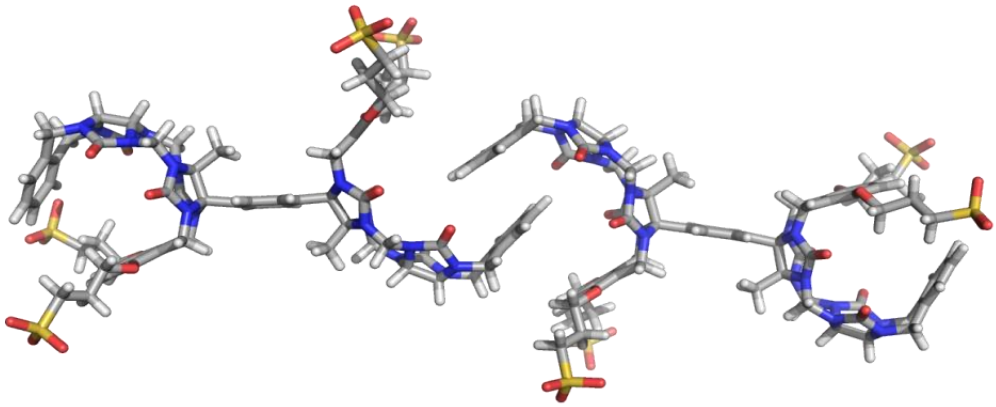

Figure 1. Optimized structure of two molecules of **4** bound together using the semi-empirical PM3 method.

The synthesis of **4** began with the reaction of glycoluril cyclic ether **1** with *o*-xylylene-protected glycoluril **5**, which was previously designed in our lab as a tool for the synthesis of glycoluril oligomers (Scheme 1) [29]. Compound **5** selectively reacted only with those two nitrogen atoms of **1** which were in the proximity of the methyl substituent, leaving the remaining two nitrogen atoms hindered by the phenylene moiety unreacted. The reaction produced compound **3** with a yield of 72%. Compound **3** also reacted with **6** to introduce the other pair of side wall-bearing sulfonate groups, which provide the final compound **4**, soluble in water. Compound **4** was prepared with a yield of 45%. The ^{1}H NMR spectra revealed the presence of two conformers of **4** (shown in Scheme 1) enabled by the rotation of clips around the phenylene unit. We previously described similar conformers for compounds **1** and **2** and studied the energy characteristics of their conformational changes [25].

Prior to investigating compound **4**, we decided to prepare and test compound **13a**, which possesses a single binding site (Scheme 2). Compound **13a** was expected to form the dimeric complex **13a**$_2$. We would be able to determine the association constant (K_a) for **13a**$_2$ and use it to estimate the strength of self-association between binding sites of **4**. The synthesis of the **13a** model compound started from phenylacetylene **7** (Scheme 2). In the first step, phenylacetylene **7** was deprotonated using *n*-butyllithium and subsequently methylated with iodomethane to give prop-1-ynylbenzene **8**. The triple bond of **8** was then oxidized using the $RuCl_3/NaIO_4$ mixture, yielding diketone **9**. Compound **9** provided glycoluril **10** after condensation with urea in 0.3 M HCl, and the glycoluril was transformed into cyclic ether **11** by reaction with formaldehyde in 9 M HCl. Condensation of **11** with **5** (for structure, see Scheme 1) in $MeSO_3H$ provided glycoluril dimer **12**. Compound **12** was transformed into the water-soluble glycoluril dimer **13a** by reaction with **6**.

The self-association of **13a** to dimer **13a**$_2$ was investigated using dilution experiments using NMR and ITC in pure D_2O/water and in 20 mM and 100 mM phosphate buffer (Table 1). The association constant of dimerization (K_a) in the absence of buffer determined by NMR ($(2.6 \pm 0.1) \times 10^3$ M^{-1}) and ITC ($(2.1 \pm 0.2) \times 10^3$ M^{-1}) were in excellent agreement. The K_a values for **13a**$_2$ measured in the presence of 20 mM and 100 mM phosphate buffer were approximately two and four times higher than those measured in pure water (Table 1). The presence of salt in the solution improved the dimerization of **13a**$_2$ either by strengthening the hydrophobic effect or by compensating the charge of the sulfonate groups and weakening their electrostatic repulsion.

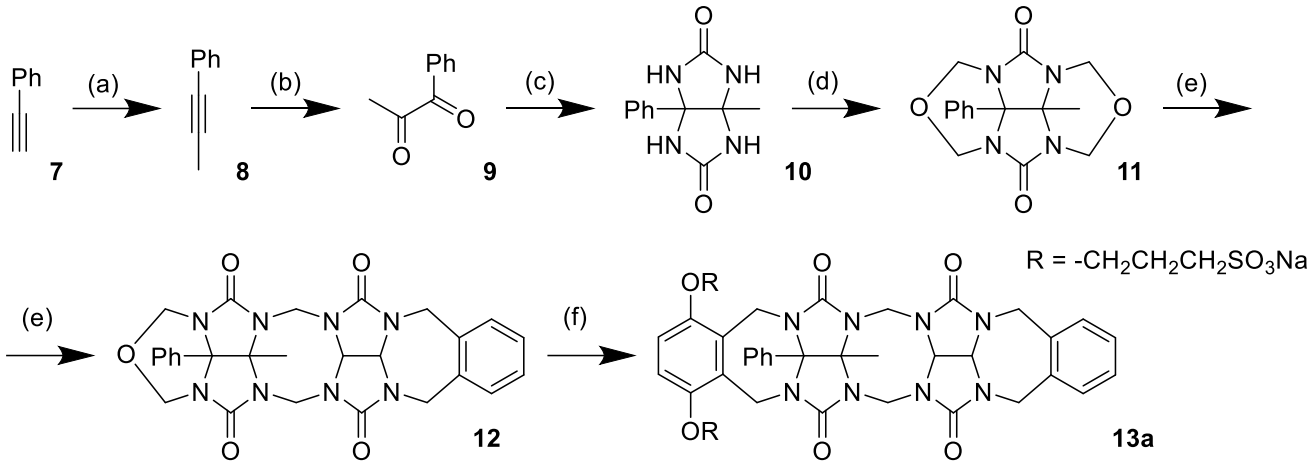

Scheme 2. Synthesis of glycoluril dimer **13a**. Reaction conditions: (**a**) 1. *n*-BuLi, THF, −78 °C, 40 h, 2. MeI, 0–25 °C, 12 h, 89%; (**b**) $RuCl_3$, $NaIO_4$, CCl_4/MeCN/water, 25 °C, 1.5 h, 74%; (**c**) urea, 0.3 M HCl, 60 °C, 24 h, 57%; (**d**) CH_2O, 9 M HCl, 25 °C, 24 h, 52%; (**e**) **5**, $MeSO_3H$, 60 °C, 4 h, 90%; (**f**) **6**, TFA/Ac_2O, 95 °C, 3 h, 51%.

The binding affinities for the dimerization of **13a** were compared to the related water-soluble glycoluril dimers **13b**–**d** (Figure 2) [10,19]. The values showed that **13a** dimerizes significantly more strongly than **13b**; however, the K_a of $\mathbf{13a}_2$ is smaller than the K_a of both $\mathbf{13c}_2$ and $\mathbf{13d}_2$ (Table 1). Observed differences were probably due to the extended repulsion between the solubilizing groups upon the self-association, which is different among these molecules. Compound **13b** has four sulfonate groups close to the binding site, which causes higher repulsion compared to **13a** with two sulfonate groups. On the other hand, the carboxylate groups of **13c** and **13d** are located on the convex side of these molecules; therefore, they are an unlikely source of repulsion that might hinder self-association.

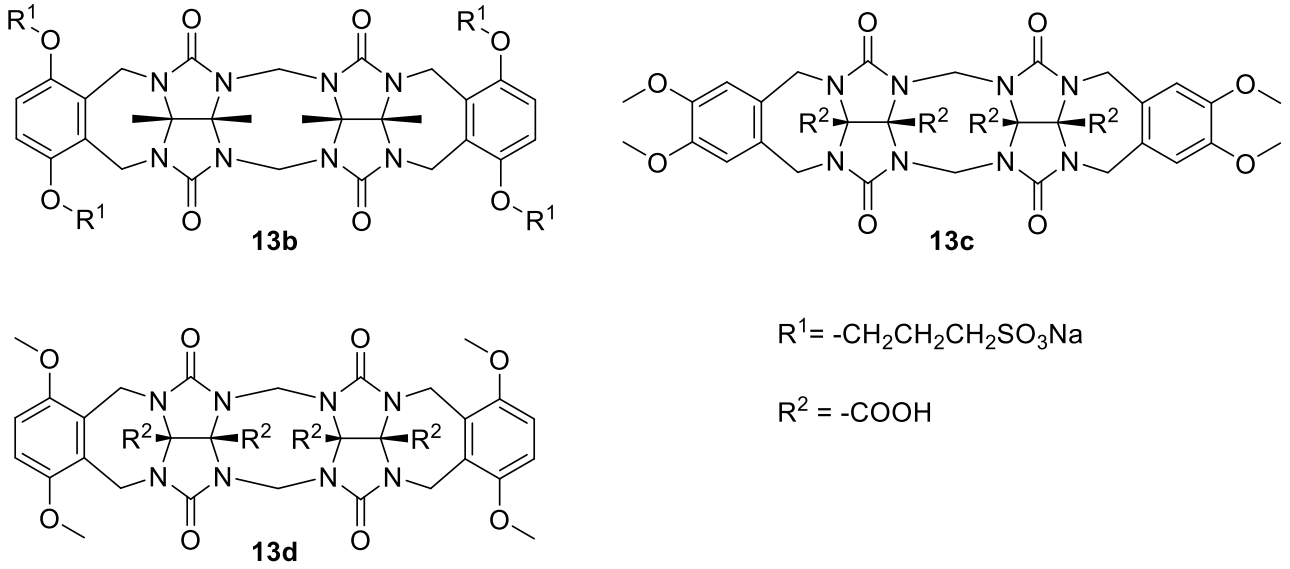

Figure 2. Structures of previously reported glycoluril dimers **13b**–**d** [10,19].

Table 1. Association constants and thermodynamic parameters of the **13a** dimer and their comparison with previously reported values for dimers of **13b** [10], **13c** [19], and **13d** [19] in water and phosphate buffer (PB) solutions. Most values were determined using ITC, values obtained by NMR titrations are marked with asterisks (*).

Glycoluril Dimer	Medium	K_a (M^{-1})	ΔG (kJ mol^{-1})	ΔH (kJ mol^{-1})	$T\Delta S$ (kJ mol^{-1})
13a	Water	$(2.6 \pm 0.1) \times 10^3$ * $(2.1 \pm 0.2) \times 10^3$	−19.3	−46.1	−27.1
	PB 20 mM	$(5.9 \pm 0.1) \times 10^3$	−21.9	−45.1	−23.3
	PB 100 mM	$(1.1 \pm 0.1) \times 10^4$	−23.4	−45.1	−21.7
13b [10]	PB 20 mM	12 *	-	-	-
13c [19]	PB 100 mM	2.6×10^4	−25.1	−14.7	10.5
13d [19]	PB 100 mM	4.2×10^4	−26.3	−19.9	6.5

ITC measurements showed that $\mathbf{13a}_2$ dimer formation is an exclusively enthalpically driven process, while entropy is unfavorable (Table 1). This contrasts with the published thermodynamic data for **13c** and **13d**, where both favorable enthalpy and entropy of dimerization were reported. Compound **13a** has two different types of aromatic side walls, the 'unsubstituted' wall originating from *o*-xylylene glycoluril and the 'substituted' wall that contains electron-donating alkoxy groups. Therefore, we assume that π-π stacking to the dimerization enthalpy of **13a** is greater than in the case of the reported compounds **13c** and **13d**, in which both aromatic walls are electron-rich due to the presence of methoxy groups. This might be the reason for the relatively high enthalpy of the $\mathbf{13a}_2$ dimer formation. Entropy compensation in **13a** dimerization, contrasting to the positive entropy term in the case of the $\mathbf{13c}_2$ and $\mathbf{13d}_2$ dimer formation, is probably due to the necessity to adopt an arrangement with the lowest electrostatic repulsion of the sulfonates. It should be noted that the above-mentioned differences among **13b–d** could also be a result of their different hydration [30,31].

Supramolecular studies performed with the model compound **13a** revealed that its dimerization occurs at a submillimolar concentration in water. Compound **4** contains very similar binding motives as **13a**. Therefore, the formation of supramolecular polymers under similar conditions was expected. We decided to monitor the formation of supramolecular polymers by measuring diffusion coefficients of **4** at various concentrations using DOSY in D_2O. The measurement gave a monotonous decrease in the diffusion coefficient with an increasing concentration of **4** (Figure 3). This trend indeed indicates that self-assembly occurred.

The degree of polymerization (n) was then determined. With the K_a of the compound of model **13a**, it is possible to predict the degree of polymerization n of **4** using the isodesmic model [32]. This model assumes that the binding sites of **13a** and **4** are essentially the same, and all the binding events occur with the same association constant. The model is described by Equation (1):

$$n = \sqrt{K_a \cdot c} \quad (1)$$

where c is the molar concentration of **4** and K_a is the dimerization constant of **13a** determined by NMR. The results presented in Figure 4 show that the length of the supramolecular polymer increases from 3.6 repeating units at 5 mM concentrations of **4** to 10 units at 40 mM concentrations of **4** in D_2O.

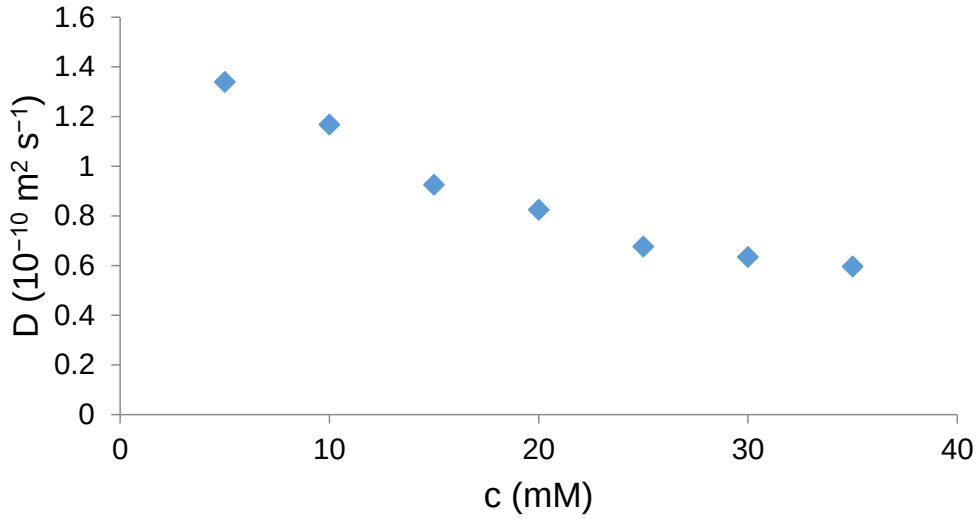

Figure 3. Diffusion coefficient of **4** versus concentration of **4** in D_2O at 30 °C.

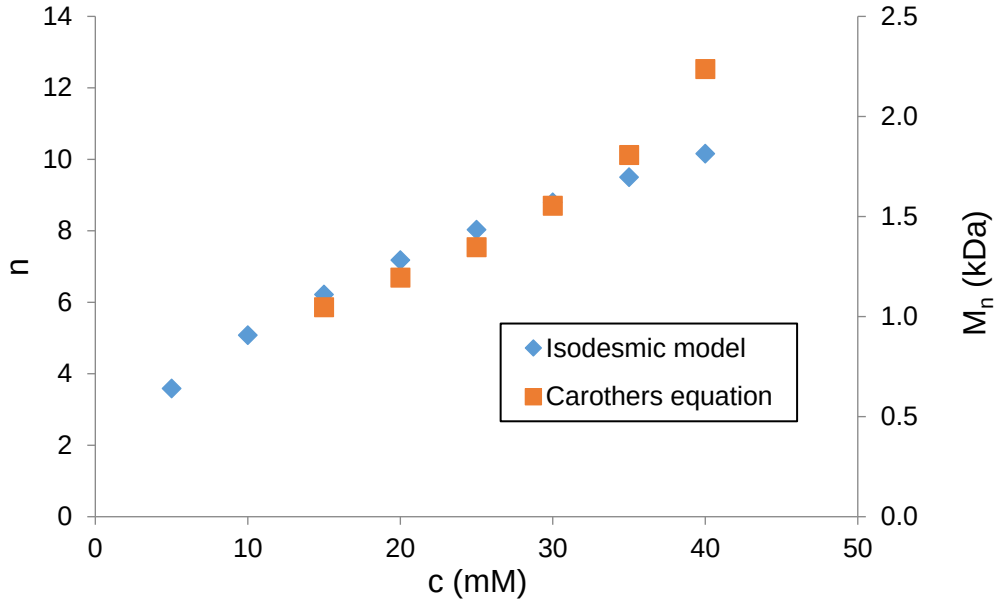

Figure 4. Degree of polymerization n and the corresponding number of average molar mass $\overline{M_n}$ of supramolecular oligomer versus the concentration of **4** in D_2O.

The second method for determining the degree of polymerization of **4** utilized NMR spectroscopy, specifically the chemical shift of protons of **4** induced by its self-association. Self-association of the **13a** model compound was necessary for it to be monitored by ^{1}H NMR (Figure 5). We particularly monitored the chemical shift of aromatic protons H1 and H2 of **13a** (for proton assignment, see Scheme 1), which shifted to lower ppm with an increasing concentration of **13a** in D_2O. From these measurements, chemical shifts corresponding to monomeric and dimeric forms of **13a** were calculated using the non-linear curve-fitting of the data. The calculation yielded the percentage of free and complexed forms of **13a** at various concentrations. The to lower ppm shift of aromatic protons similar to those of **13a** was also observed for the solution of **4** in D_2O with its increasing concentration (Figure S10). If we consider that the chemical shifts of aromatic protons in **4** and **13a** with their increasing concentrations are essentially identical, we can use data obtained from the dimerization of **13a** to calculate the chemical shifts of the free and dimeric compound **4**. Subsequently, we determined the percentage of binding sites of **4**, which undergo self-association at different concentrations (for calculation, see Supplementary Materials).

Assuming that only linear aggregates are formed, the percentage of complexed sites can be associated with the monomer conversion p the Carothers equation [33], which allows one to calculate the degree of polymerization:

$$n = \frac{1}{1-p}. \quad (2)$$

Figure 4 shows good agreement between the degrees of polymerization calculated by two different methods in the concentration range from 15 mM to 35 mM. However, at a higher concentration of **4** (>30 mM), the polymerization degree values obtained from the isodesmic model are significantly lower compared to those obtained from the Carothers equation. We assume that this deviation is due to increasing ionic strength, which influences the self-association process. As compound **4** is a sodium salt of sulfonic acid, the ionic strength increases with the increasing concentration of **4**. The Carothers equation uses data of chemical shift from real solutions; thus, calculated values also reflect the increase in ionic strength. On the other hand, the isodesmic model presumes that self-association affinity is concentration independent, which causes deviation of calculated values from those obtained by Carothers equation above 30 mM of **4**.

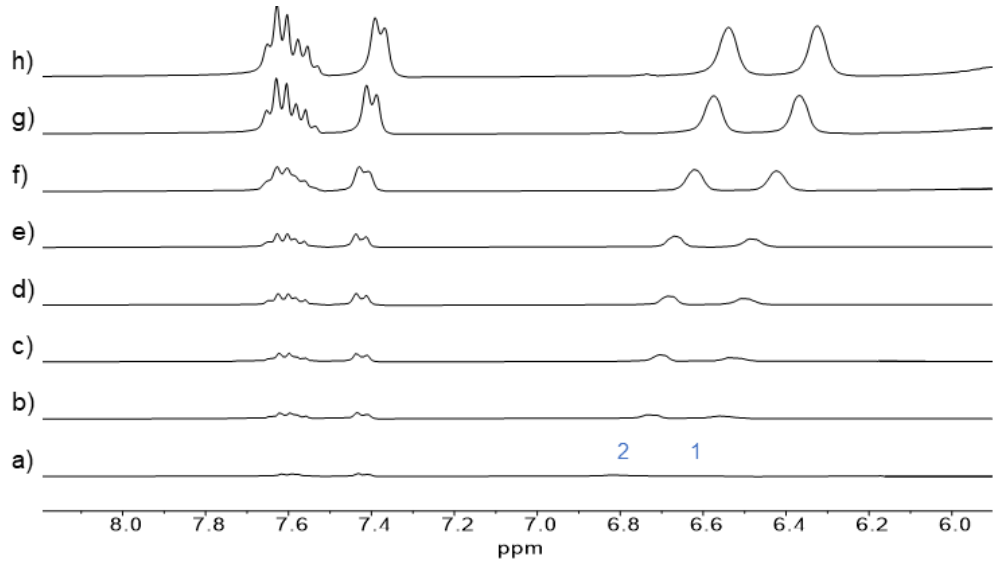

Figure 5. Partial NMR spectra (300 MHz, D_2O) of **13a** at various concentrations. Highlighted signals were used for the calculation of the degree of polymerization. Concentrations: (**a**) 1 mM, (**b**) 2 mM, (**c**) 3 mM, (**d**) 4 mM, (**e**) 5 mM, (**f**) 10 mM, (**g**) 15 mM, and (**h**) 20 mM.

3. Experimental Section

All chemicals were purchased from commercial suppliers and used without further purification. THF was dried over 4 Å molecular sieves. NMR spectra were recorded on a Bruker Avance 300 spectrometer with a working frequency of 300.13 MHz for ^{1}H and 75.48 MHz for ^{13}C or a Bruker Avance 500 spectrometer with a working frequency of 500.13 MHz for ^{1}H and 125.77 MHz for ^{13}C. Both spectrometers were equipped with a BBFO probe. NMR spectra were recorded in D_2O, DMSO-d_6, or 95% DCOOD. Chemical shifts are provided in parts per million (ppm), and coupling constants (J) are presented in Hertz (Hz). The multiplicities of signals are reported as singlet (s), doublet (d), triplet (t), or multiplet (m). Data from the NMR titration experiments were analyzed by non-linear regression using an appropriate binding model. HypNMR2008 software was used for the analysis. HR-MS spectra were recorded on an Agilent 6224 Accurate-Mass TOF mass spectrometer. Samples were ionized by electrospray ionization (ESI) or by atmospheric pressure chemical ionization (APCI). Melting points were determined using an MPM-HV2 melting point apparatus in an open-end capillary tube.

ITC experiments were performed on a VP-ITC instrument (Microcal, GEHealthcare). Experiments were carried out at 303.15 ± 0.1 K. In a typical experiment, 29 aliquots (10 µL) of 5.0 mM solution of **13a** were injected into ITC cells containing either ultrapure water, 20 mM, or 100 mM sodium phosphate-buffered water at pH = 7.0. Integrated heat effects were analyzed by non-linear regression using a dissociation model. Microcal Origin 7 software was used for the analysis.

3.1. Synthesis of Compound **3**

Cyclic ether **1** [25] (1.112 g, 2.01 mmol) was dissolved in methanesulfonic acid (17 mL). *o*-Xylyleneglycoluril **5** (1.014 g, 4.15 mmol) was added and the solution was stirred under a nitrogen atmosphere at 60 °C for 4 h. The solution was allowed to cool down to RT, and it was poured into acetone (100 mL). The resulting precipitate was collected by filtration and washed with acetone. The crude product was dissolved in formic acid (15 mL) and precipitated with water (100 mL). The precipitate was collected by filtration and washed with water, acetone, and diethyl ether to afford compound 3 as a white powder (1.622 g, 72%).

NMR spectra of this compound indicate the presence of distinct conformers. ^{1}H NMR (500 MHz, 95% DCOOD): δ (ppm) = 7.69 (s, 4H); 7.38 (m, 4H); 7.31 (m, 4H); 5.93 (d, J = 8.1 Hz, 2H); 5.89 (d, J = 16.0 Hz, 4H); 5.77 (d, J = 8.1 Hz, 2H); 5.49 (d, J = 11.0 Hz, 4H); 4.87 (d, J = 15.9 Hz, 4H); 4.70 (d, J = 15.9 Hz, 4H); 4.59 (m, 4H); 4.53 (m, 4H); 1.43, 1.39 (s, 6H). ^{13}C NMR (125 MHz, 95% DCOOD): δ (ppm) = 157.44; 157.17; 136.65; 135.16; 134.96; 129.48; 129.10; 129.07; 128.44; 79.42; 78.25; 71.81; 70.53; 70.17; 48.56; 45.66; 17.70. HR-MS (MALDI, HCCA): calculated: $[C_{48}H_{46}N_{16}O_{10} + H]^{+}$ = 1007.3656 observed 1007.3667. Melting point > 300 °C.

3.2. Synthesis of Compound **4**

Compound **3** (1.401 g, 1.39 mmol) and compound **6** (2.251 g, 5.65 mmol) were dissolved in a mixture of TFA (15 mL) and acetic anhydride (15 mL). The solution was heated to 95 °C for 3 h. Solvents were removed by rotary evaporation, and the resulting solid was triturated with methanol (200 mL). The crude product was dissolved in water (20 mL) and precipitated with acetone (150 mL). The precipitation was repeated twice with the same volume of solvents. The precipitate was then again dissolved in water (20 mL); the pH of the solution was adjusted to 7 using 1 M NaOH, and the water was removed by rotary evaporation. The resulting solid was washed with methanol and diethyl ether and dried *in vacuo* to afford compound **4** as a beige solid (1.101 g, 45%).

NMR spectra of this compound indicate the presence of distinct conformers. ^{1}H NMR (300 MHz, DMSO-d_6): δ (ppm) = 7.46, 7.39 (s, 4H); 7.22 (m, 8H); 5.54 (m, 8H); 5.36 (m, 4H); 4.57 (m, 8H); 4.13 (m, 4H); 3.92 (m, 8H); 3.80 (m, 4H); 2.62 (m, 8H); 2.00 (m, 8H); 1.08 (m, 6H). ^{13}C NMR (125 MHz, DMSO-d_6): δ (ppm) = 155.00; 154.89; 149.87; 137.38; 134.78, 134.69; 129.24; 128.73; 127.58; 127.21; 127.03; 113.37; 83.27, 83.09; 77.54; 77.18; 68.81; 68.35; 48.33; 48.29; 45.15; 36.02; 25.55; 17.81. HR-MS (ESI): calculated: $[C_{72}H_{74}N_{16}Na_4O_{24}S_4 + 2\ Na]^{2+}$ = 906.1660 observed = 906.1593. Melting point > 300 °C.

3.3. Synthesis of Compound **8**

Phenylacetylene **7** (5.013 g, 48.95 mmol) was dissolved in anhydrous THF (150 mL) under a nitrogen atmosphere, the solution was cooled to −78 °C, and *n*-butyllithium (1.6 M in hexanes, 32.0 mL, 51.20 mmol) was added dropwise. The reaction mixture was stirred for 40 min, and it was heated up to 0 °C. Iodomethane (6.0 mL, 96.37 mmol) was added, and the reaction mixture was allowed to warm to room temperature and was stirred overnight. The reaction mixture was then treated with water (100 mL); the product was extracted with CH_2Cl_2 (3 × 80 mL); combined organic extracts were washed with water (40 mL) and brine (40 mL) dried over anhydrous $MgSO_4$, and the solvent was removed by rotary evaporation to afford **8** as a yellowish oil (5.031 g, 89%).

The spectroscopic data matches those reported in the literature [34].

3.4. Synthesis Compound **9**

Alkyne **8** (4.721 g, 50.0 mmol) was dissolved in a mixture of CCl_4 (61 mL) and CH_3CN (61 mL). A mixture of $NaIO_4$ (25.94 g, 121.3 mmol), $NaHCO_3$ (0.270 g, 3.2 mmol), and $MgSO_4$ (1.220 g, 10.1 mmol) in water (82 mL) was added to the solution. Aqueous 0.01 M $RuCl_3$ (14 mL, 0.14 mmol) was added, and the reaction mixture was stirred at room temperature for 1.5 h. The mixture was diluted with ethyl acetate (400 mL), and the organic phase was separated from the precipitated salts by decantation. The organic phase was dried over $MgSO_4$, filtered and evaporated. The product was purified by silica gel column chromatography using ethyl acetate as a mobile phase to give compound **9** as a yellow oil (5.47 g, 74%).

The spectroscopic data matches those reported in the literature [35].

3.5. Synthesis of Glycoluril **10**

Diketone **9** (4.60 g, 31.0 mmol) was dissolved in 0.3 M HCl, urea (7.6 g, 12.7 mmol) was added, and the mixture was stirred at 60 °C for 24 h. The suspension was filtered and the solid product was washed with water, acetone, and diethyl ether to afford glycoluril **10** as a white powder (4.102 g, 57%).

The spectroscopic data matches those reported in the literature [36].

3.6. Synthesis of Compound **11**

Paraformaldehyde (2.55 g, 85.0 mmol) was dissolved in 9 M HCl (100 mL) at 60 °C; the solution was cooled down to room temperature. Glycoluril **10** (3.854 g, 16.6 mmol) was added, and the solution was stirred for 24 h. Water (100 mL) was then added to the mixture, and it was stirred for another 12 h. The resulting precipitate was collected by filtration, washed with water and dried *in vacuo* to provide ether **11** as a white powder (2.751 g, 52%).

The spectroscopic data matches those reported in the literature [36].

3.7. Synthesis of Compound **12**

Cyclic ether **11** (2.451 g, 7.64 mmol) was dissolved in methanesulfonic acid (25 mL). *o*-Xylyleneglycoluril **5** (1.956 g, 8.02 mmol) was added, and the solution was stirred under a nitrogen atmosphere at 60 °C for 4 h. The solution cooled down to room temperature, and it was poured into water (100 mL). The resulting precipitate was collected by filtration, washed with water, and dried *in vacuo* to afford compound **12** as a white powder (3.804 g, 90%).

^{1}H NMR (300 MHz, DMSO-d_6): δ (ppm) = 7.50 (m, 3H); 7.36 (m, 2H); 7.27 (m, 4H,) 5.66 (d, J = 8.1 Hz, 1H); 5.59 (d, J = 8.1 Hz, 1H); 5.56 (d, J = 15.2 Hz, 2H); 5.25 (d, J = 11.00 Hz, 2H); 4.65 (d, J = 15.6 Hz, 2H); 4.59 (d, J = 15.6 Hz, 2H); 4.37 (d, J = 11.00 Hz, 2H); 4.24 (d, J = 15.2 Hz, 2H); 1.18 (s, 3H). ^{13}C NMR (125 MHz, DMSO-d_6): δ (ppm) = 155.01; 154.64; 137.64; 133.75; 129.63; 129.19; 129.07; 127.65; 127.56; 77.98; 76.52; 71.33; 68.73; 68.61; 48.50; 45.07; 17.87. HR-MS (APCI): calculated: $[C_{27}H_{26}N_8O_5 + Cl]^-$ = 577.1720, observed = 577.1719. Melting point > 290 °C (decomposition).

3.8. Synthesis of Compound **13a**

Compound **12** (3.022 g, 5.56 mmol) and compound **6** (4.507 g, 11.31 mmol) were dissolved in a mixture of TFA (30 mL) and acetic anhydride (30 mL). The solution was heated to 95 °C for 3 h. Solvents were removed by rotary evaporation, and the resulting solid was triturated with methanol (500 mL). The crude product was dissolved in water (55 mL) and precipitated with acetone (400 mL). The precipitate was then again dissolved in water (30 mL); the pH of the solution was adjusted to 7 using 1 M NaOH, and the water was removed by rotary evaporation. The resulting solid was washed with methanol and diethyl ether and dried *in vacuo* to afford compound **13a** as a yellowish solid (2.621 g, 51%).

^{1}H NMR (500 MHz, DMSO-d_6): δ (ppm) = 7.54 (t, J = 7.7 Hz, 2H); 7.46 (t, J = 7.4 Hz, 1H); 7.29 (d, J = 7.5 Hz, 2H); 7.23 (m, 2H); 7.19 (m, 2H); 6.74 (s, 2H); 5.57, (d, J = 8.2 Hz, 1H); 5.50 (d, J = 15.2 Hz, 2H); 5.49 (d, J = 8.2 Hz, 1H); 5.38 (d, J = 15.7 Hz, 2H); 4.59 (d,

J = 15.5 Hz, 2H); 4.53 (d, J = 15.5 Hz, 2H); 4.12 (d, J = 15.2 Hz, 2H); 3.91 (m, 4H); 3.72 (d, J = 15.7 Hz, 2H); 2.65 (m, 2H); 2.59 (m, 2H); 1.99 (m, 4H); 1.06 (s, 3H). ^{13}C NMR (125 MHz, DMSO-d_6): δ (ppm) = 154.91; 154.84; 149.92; 137.33; 133.47; 129.45; 129.32; 129.24; 127.72; 127.61; 127.17; 113.55; 83.31; 77.32; 68.83; 68.54; 48.40; 48.28; 45.18; 35.86; 25.69; 17.82. HR-MS (ESI): calculated: $[C_{39}H_{40}N_8Na_2O_{12}S_2\text{-}2\ Na + H]^-$ = 877.2291, observed: = 877.2289. Melting point > 300 °C.

4. Conclusions

In conclusion, we synthesized the glycoluril dimer **13a** and its doubled analogue **4** and investigated their ability to self-associate in an aqueous environment. Compound **13a** forms discrete dimeric complexes **13a**$_2$, with the stability of $(2.6 \pm 0.1) \times 10^3$ and $(2.1 \pm 0.2) \times 10^3$ M^{-1} in water as determined by NMR and ITC. It was also discovered that the enhancement of the ionic strength of the solution makes the self-association of **13a** more favorable. Compound **4** undergoes self-association in water resulting in the formation of supramolecular oligomers, which was indicated by the decrease in the diffusion coefficient with the increasing concentration of **4**. Polymerization degree values estimated using the Carothers equation and isodesmic model were in good agreement at a lower concentration (15 to 35 mM). At a higher concentration, the determined polymerization degree was higher than that calculated by the Carothers equation, showing the influence of the ionic strength on the self-association process.

Supplementary Materials: The following supporting information can be downloaded at: https://www.mdpi.com/article/10.3390/chemistry4030053/s1, Figures S1–S8: ^{1}H and ^{13}C NMR spectra of new compounds; Figures S9 and S10: Concentration dependent ^{1}H NMR spectra of **4** and **13a**; Figures S11 and S12: ITC titrations to determine dimerization constants of **13a**; Figures S13–S19: DOSY spectra of **4** at different concentrations; Figure S20: Capped stick representation of conformers of **4**; Tables S1 and S2: Chemical shifts of free and complexed **13a** a **4**; Table S3: Geometry of the dimer of **4** optimized at PM3 semi-empirical level of theory.

Author Contributions: Synthesis and characterization of new compounds, self-association studies: J.S.; project conception and supervision: V.Š.; manuscript preparation and editing: J.S., V.Š. All authors have read and agreed to the published version of the manuscript.

Funding: This research was funded by the Czech Science Foundation (No. GA20-13922S), the RECETOX Research Infrastructure (No. LM2018121), financed by the Ministry of Education, Youth and Sports, and the Operational Programme Research, Development and Education (the CETOCOEN EXCELLENCE project No. CZ.02.1.01/0.0/0.0/17_043/0009632) for supportive background. This project was supported by the European Union's Horizon 2020 Research and Innovation Programme under grant agreement No. 857560. We acknowledge the Proteomic Core Facility of CIISB, Instruct-CZ Centre, supported by MEYS CR (LM2018127).

Institutional Review Board Statement: Not applicable.

Informed Consent Statement: Not applicable.

Data Availability Statement: Data underpinning the work in this paper that is not already included in Supplementary Materials is available on request from the corresponding author.

Conflicts of Interest: The authors declare no conflict of interest. This publication reflects only the author's view and the funders are not responsible for any use that may be made of the information it contains. The funders had no role in the design of the study; in the collection, analyses, or interpretation of data; in the writing of the manuscript; or in the decision to publish the results.

References

1. Whitesides, G.M. Self-Assembly at All Scales. *Science* **2002**, *295*, 2418–2421. [CrossRef]
2. Chen, L.; Chen, Q.; Wu, M.; Jiang, F.; Hong, M. Controllable Coordination-Driven Self-Assembly: From Discrete Metallocages to Infinite Cage-Based Frameworks. *Acc. Chem. Res.* **2015**, *48*, 201–210. [CrossRef]
3. Boekhoven, J.; van Rijn, P.; van Esch, J.H. Self-Assembly of Facial Amphiphiles in Water. In *Supramolecular Chemistry*; Gale, P.A., Steed, J.W., Eds.; John Wiley & Sons, Ltd.: Chichester, UK, 2012; p. smc144. [CrossRef]

4. Lagona, J.; Mukhopadhyay, P.; Chakrabarti, S.; Isaacs, L. The Cucurbit[*n*]Uril Family. *Angew. Chem. Int. Ed.* **2005**, *44*, 4844–4870. [CrossRef] [PubMed]
5. Lizal, T.; Sindelar, V. Bambusuril Anion Receptors. *Isr. J. Chem.* **2018**, *58*, 326–333. [CrossRef]
6. Rebek, J. Reversible Encapsulation and Its Consequences in Solution. *Acc. Chem. Res.* **1999**, *32*, 278–286. [CrossRef]
7. Rowan, A.E.; Elemans, J.A.A.W.; Nolte, R.J.M. Molecular and Supramolecular Objects from Glycoluril. *Acc. Chem. Res.* **1999**, *32*, 995–1006. [CrossRef]
8. Sijbesma, R.P.; Kentgens, A.P.M.; Lutz, E.T.G.; van der Maas, J.H.; Nolte, R.J.M. Binding Features of Molecular Clips Derived from Diphenylglycoluril. *J. Am. Chem. Soc.* **1993**, *115*, 8999–9005. [CrossRef]
9. Ma, D.; Zavalij, P.Y.; Isaacs, L. Acyclic Cucurbit[*n*]Uril Congeners Are High Affinity Hosts. *J. Org. Chem.* **2010**, *75*, 4786–4795. [CrossRef]
10. Gilberg, L.; Zhang, B.; Zavalij, P.Y.; Sindelar, V.; Isaacs, L. Acyclic Cucurbit[*n*]Uril-Type Molecular Containers: Influence of Glycoluril Oligomer Length on Their Function as Solubilizing Agents. *Org. Biomol. Chem.* **2015**, *13*, 4041–4050. [CrossRef] [PubMed]
11. Ganapati, S.; Isaacs, L. Acyclic Cucurbit[*n*]Uril-Type Receptors: Preparation, Molecular Recognition Properties and Biological Applications. *Isr. J. Chem.* **2018**, *58*, 250–263. [CrossRef]
12. Brady, K.G.; Gilberg, L.; Sigwalt, D.; Bistany-Riebman, J.; Murkli, S.; Klemm, J.; Kulhánek, P.; Šindelář, V.; Isaacs, L. Conformationally Mobile Acyclic Cucurbit[*n*]Uril-Type Receptors Derived from an S-Shaped Methylene Bridged Glycoluril Pentamer. *Supramol. Chem.* **2020**, *32*, 479–494. [CrossRef] [PubMed]
13. Zhang, B.; Zavalij, P.Y.; Isaacs, L. Acyclic CB[*n*]-Type Molecular Containers: Effect of Solubilizing Group on Their Function as Solubilizing Excipients. *Org. Biomol. Chem.* **2014**, *12*, 2413–2422. [CrossRef] [PubMed]
14. She, N.; Moncelet, D.; Gilberg, L.; Lu, X.; Sindelar, V.; Briken, V.; Isaacs, L. Glycoluril-Derived Molecular Clips Are Potent and Selective Receptors for Cationic Dyes in Water. *Chem. Eur. J.* **2016**, *22*, 15270–15279. [CrossRef]
15. Gosecki, M.; Urbaniak, M.; Gostynski, B.; Gosecka, M. Influence of Glycoluril Molecular Clip Isomerization on the Mechanisms of Resorcinol Molecule Complexation. *J. Phys. Chem. C* **2020**, *124*, 8401–8410. [CrossRef]
16. Lu, X.; Isaacs, L. Synthesis and Recognition Properties of Enantiomerically Pure Acyclic Cucurbit[*n*]Uril-Type Molecular Containers. *Org. Lett.* **2015**, *17*, 4038–4041. [CrossRef] [PubMed]
17. Liu, W.; Ai, H.; Meng, Z.; Isaacs, L.; Xu, Z.; Xue, M.; Yan, Q. Interactions between Acyclic CB[*n*]-Type Receptors and Nitrated Explosive Materials. *Chem. Commun.* **2019**, *55*, 10635–10638. [CrossRef] [PubMed]
18. Lu, X.; Zebaze Ndendjio, S.A.; Zavalij, P.Y.; Isaacs, L. Acyclic Cucurbit[*n*]Uril-Type Receptors: Optimization of Electrostatic Interactions for Dicationic Guests. *Org. Lett.* **2020**, *22*, 4833–4837. [CrossRef] [PubMed]
19. Isaacs, L.; Witt, D.; Lagona, J. Self-Association of Facially Amphiphilic Methylene Bridged Glycoluril Dimers. *Org. Lett.* **2001**, *3*, 3221–3224. [CrossRef] [PubMed]
20. Ghosh, S.; Wu, A.; Fettinger, J.C.; Zavalij, P.Y.; Isaacs, L. Self-Sorting Molecular Clips. *J. Org. Chem.* **2008**, *73*, 5915–5925. [CrossRef]
21. Ma, D.; Zhang, B.; Hoffmann, U.; Sundrup, M.G.; Eikermann, M.; Isaacs, L. Acyclic Cucurbit[*n*]Uril-Type Molecular Containers Bind Neuromuscular Blocking Agents In Vitro and Reverse Neuromuscular Block In Vivo. *Angew. Chem. Int. Ed.* **2012**, *51*, 11358–11362. [CrossRef] [PubMed]
22. Ganapati, S.; Grabitz, S.D.; Murkli, S.; Scheffenbichler, F.; Rudolph, M.I.; Zavalij, P.Y.; Eikermann, M.; Isaacs, L. Molecular Containers Bind Drugs of Abuse in Vitro and Reverse the Hyperlocomotive Effect of Methamphetamine in Rats. *ChemBioChem* **2017**, *18*, 1583–1588. [CrossRef] [PubMed]
23. Schenning, A.P.H.J.; de Bruin, B.; Feiters, M.C.; Nolte, R.J.M. Molecular Golf Balls: Vesicles from Bowl-Shaped Host Molecules. *Angew. Chem. Int. Ed. Engl.* **1994**, *33*, 1662–1663. [CrossRef]
24. van Nunen, J.L.M.; Stevens, R.S.A.; Picken, S.J.; Nolte, R.J.M. Tunable Supramolecular Structures from Clips and Baskets Derived from Glycoluril. *J. Am. Chem. Soc.* **1994**, *116*, 8825–8826. [CrossRef]
25. Sokolov, J.; Lizal, T.; Sindelar, V. Dimeric Molecular Clips Based on Glycoluril. *New J. Chem.* **2017**, *41*, 6105–6111. [CrossRef]
26. Wu, A.; Mukhopadhyay, P.; Chakraborty, A.; Fettinger, J.C.; Isaacs, L. Molecular Clips Form Isostructural Dimeric Aggregates from Benzene to Water. *J. Am. Chem. Soc.* **2004**, *126*, 10035–10043. [CrossRef]
27. Reek, J.N.H.; Elemans, J.A.A.W.; de Gelder, R.; Beurskens, P.T.; Rowan, A.E.; Nolte, R.J.M. Self-Association and Self-Assembly of Molecular Clips in Solution and in the Solid State. *Tetrahedron* **2003**, *59*, 175–185. [CrossRef]
28. Isaacs, L.; Fettinger, J.C. Design, Synthesis and Self-Association Behavior of Water Soluble Self Complementary Facial Amphiphiles. *Chem. Commun.* **1999**, *24*, 2549–2550. [CrossRef]
29. Stancl, M.; Hodan, M.; Sindelar, V. Glycoluril Trimers: Selective Synthesis and Supramolecular Properties. *Org. Lett.* **2009**, *11*, 4184–4187. [CrossRef]
30. Biedermann, F.; Uzunova, V.D.; Scherman, O.A.; Nau, W.M.; De Simone, A. Release of High-Energy Water as an Essential Driving Force for the High-Affinity Binding of Cucurbit[*n*]Urils. *J. Am. Chem. Soc.* **2012**, *134*, 15318–15323. [CrossRef]
31. Kubik, S. When Molecules Meet in Water-Recent Contributions of Supramolecular Chemistry to the Understanding of Molecular Recognition Processes in Water. *ChemistryOpen* **2022**, *11*, e202200028. [CrossRef]
32. Isla, H.; Pérez, E.M.; Martín, N. High Degree of Polymerization in a Fullerene-Containing Supramolecular Polymer. *Angew. Chem. Int. Ed.* **2014**, *53*, 5629–5633. [CrossRef] [PubMed]

33. Gao, L.; Zhang, Z.; Dong, S.; Xue, M. Formation of a Copillar[5]Arene-Based Supramolecular Polymer in Solution and in the Solid State. *Macromol. Rapid Commun.* **2014**, *35*, 987–991. [CrossRef] [PubMed]
34. Unoh, Y.; Hirano, K.; Satoh, T.; Miura, M. An Approach to Benzophosphole Oxides through Silver- or Manganese-Mediated Dehydrogenative Annulation Involving C—C and C—P Bond Formation. *Angew. Chem. Int. Ed.* **2013**, *52*, 12975–12979. [CrossRef]
35. Guha, S.; Rajeshkumar, V.; Kotha, S.S.; Sekar, G. A Versatile and One-Pot Strategy to Synthesize α-Amino Ketones from Benzylic Secondary Alcohols Using *N* -Bromosuccinimide. *Org. Lett.* **2015**, *17*, 406–409. [CrossRef] [PubMed]
36. Vinciguerra, B.; Cao, L.; Cannon, J.R.; Zavalij, P.Y.; Fenselau, C.; Isaacs, L. Synthesis and Self-Assembly Processes of Monofunctionalized Cucurbit[7]Uril. *J. Am. Chem. Soc.* **2012**, *134*, 13133–13140. [CrossRef] [PubMed]